GA–A22393

THE SPHERICAL TORUS APPROACH TO MAGNETIC FUSION DEVELOPMENT

by
R.D. STAMBAUGH, V.S. CHAN, P.A. ANDERSON, C.B. BAXI,
R.W. CALLIS, H.K. CHIU, C.B. FOREST, R. HONG, T.K. JENSEN, L.L. LAO,
J.A. LEUER, M.A. MAHDAVI, R.L. MILLER, A. NEREM, R. PRATER,
P.A. POLITZER, M.J. SCHAFFER, D.L. SEVIER, T.S. TAYLOR,
A.D. TURNBULL, and C.P.C. WONG

JUNE 1996

GA–A22388

THE SPHERICAL TORUS APPROACH TO MAGNETIC FUSION DEVELOPMENT

by
R.D. STAMBAUGH, V.S. CHAN, P.A. ANDERSON, C.B. BAXI, R.W. CALLIS, H.K. CHIU, C.B. FOREST, R. HONG, T.K. JENSEN, L.L. LAO, J.A. LEUER, M.A. MAHDAVI, R.L. MILLER, A. NEREM, R. PRATER, P.A. POLITZER, M.J. SCHAFFER, D.L. SEVIER, T.S. TAYLOR, A.D. TURNBULL, and C.P.C. WONG

This is a preprint of a paper to be presented at the Twelfth Topical Meeting on Technology of Fusion Energy, June 16–20 1996, Reno, Nevada, and to be published in *The Proceedings.*

GA PROJECT 4437
JUNE 1996

THE SPHERICAL TORUS APPROACH TO MAGNETIC FUSION DEVELOPMENT

R.D. Stambaugh, V.S. Chan, P.A. Anderson, C.B. Baxi, R.W. Callis, H.K. Chiu, C.B. Forest, R. Hong, T.K. Jensen, L.L. Lao, J.A. Leuer, M.A. Mahdavi, R.L. Miller, A. Nerem, R. Prater, P.A. Politzer, M.J. Schaffer, D.L. Sevier, T.S. Taylor, A.D. Turnbull, and C.P.C. Wong

General Atomics
P.O. Box 85608
San Diego, California 92186-9784
(619)455-4153

ABSTRACT

The low aspect ratio tokamak or spherical torus (ST) approach offers the two key elements needed to enable magnetic confinement fusion to make the transition from a government-funded research program to the commercial marketplace: a low cost, low power, small size market entry vehicle and a strong economy of scale in larger devices. Within the ST concept, a very small device (A = 1.4, major radius about 1 m, similar size to the DIII–D tokamak) could be built that would produce ~800 MW thermal, 250 MW net electric, and would have a gain, defined as Q_{PLANT} = (gross electric power/recirculating power), of about 2. Such a device would have all the operating systems and features of a power plant and would therefore be acceptable as a pilot plant, even though the cost of electricity would not be competitive. The ratio of fusion power to copper TF coil dissipation rises quickly with device size (like R^4) and can lead to 3 GW thermal power plants with Q_{PLANT} = 4–5 but which remain a factor 3 smaller than superconducting tokamak power plants. Power plants of the scale of ITER might be able to burn the advanced fuel D-He^3.

I. INTRODUCTION

The principal need in the development of magnetic fusion energy as a domestic source of electric power in the United States is defining a low cost market entry vehicle that would make enough electric power to attract commercial interest. The spherical tokamak (ST) approach appears to provide an answer. The ST approach minimizes the size of a tokamak power core by discarding all non-essential components from the inner side of the plasma: no inboard blanket or shield, no inboard poloidal coil (PF) systems, no Ohmic heating (OH) solenoid. The resulting systems lie in the family of low aspect ratio tokamaks, with aspect ratio A ($A = R_0/a$) generally considered less than 1.5. The only customary tokamak component that remains is a single turn copper toroidal field (TF) coil centerpost. Consequently, the ST shrinks to the absolute minimum size and cost tokamak fusion system.

The advantages of the spherical tokamak approach have been discussed for many years (1,2). In recent years, interest in the ST approach has grown rapidly, spawning a new experimental machine proposals (4,5,6). Reference (7) is a valuable review of the field. Some studies projecting the ST approach to burning plasma devices have appeared (8,9).

The physics key to the attractiveness of the ST approach is in the order unity beta values promised by the combination of high elongation and low aspect ratio. We find that the projected beta values and power densities are sufficiently high that limits on the neutron wall loading of the blankets are the determining factor in the machine size. The fusion power that can be produced far exceeds the Ohmic losses in the copper TF coil. Because there is no OH transformer in the ST approach, the devices are of necessity steady-state with full non-inductive current drive. Self-driven current fractions up to 90% are expected. The remaining requirement for current drive power and the TF coil Ohmic power remain small enough to project systems with reasonable levels of plant recirculating power. A very large advantage is the copper TF coil which can be jointed and allows a simple path to full dissassembly and replacement of all components,

including the centerpost. Estimates of the increase in resistivity of the centerpost from neutron induced transmutation indicate the possibility of a multi-year lifetime before replacement. The absence of an inboard blanket is a negligible penalty in tritium breeding or power production since the centerpost intercepts a small fraction of the fusion neutrons (2). The single turn nature of the centerpost requires unusual power supplies (few volts, MA currents) which appear possible. The high power density is a challenge to the divertor.

In this paper, we find that, within this ST concept, it appears (Fig. 1) possible to design a pilot plant that would only be the size of the present DIII–D tokamak and still produce some net electric power. At double the size of the pilot plant we have identified full 1–2 GW net electric power plants with acceptable economics. A full account of our work can be found in Ref. (10).

II. POWER GAIN

The key issue for the low aspect ratio tokamak approach to a fusion power plant is whether a large excess of fusion power P_F can be produced relative to the resistive power in the TF centerpost P_c. We will calculate a "centerpost gain" $\left(P_F/P_c\right)$ and look at optimizations.

The toroidal coil (TF) centerpost is a straight cylinder of radius R_c and height h_c. No other space allowance is taken on the inboard side. We discuss the machine performance in terms of the independent variables R_c, aspect ratio A, and elongation κ, since the centerpost power consumption is the main issue and we are interested in optimization of performance versus A The plasma major radius R_0 and minor radius a are then derived quantities.

Using standard forms for the D-T fusion reactivity (11), the optimum D-T mix, $n_D = n_T = 1/2\, n_e$, and parabolic profiles with exponents $S_n = 0$ (flat n) and $S_T = 2$ (peaked T), we can express the alpha power as

$$P_\alpha = 2.06 \times 10^{-4}\, V n_{020}^2\, T_0^2 \quad . \qquad (1)$$

where n_{020} is the central density in 10^{20} m^{-3} and T_0 is the central temperature in keV. $P_F = 5\, P_\alpha$. To express P_F in terms of the volume average plasma β, we use the toroidal β_T and the vacuum toroidal field B_T at the geometric center of the plasma in order to keep contact with the β-limit scaling for higher aspect ratio tokamaks (12)

$$\beta_N \equiv \beta_T \Big/ \left(I_p / aB_T\right) \quad (\%,\mathrm{MA,m,T}) \quad , \qquad (2)$$

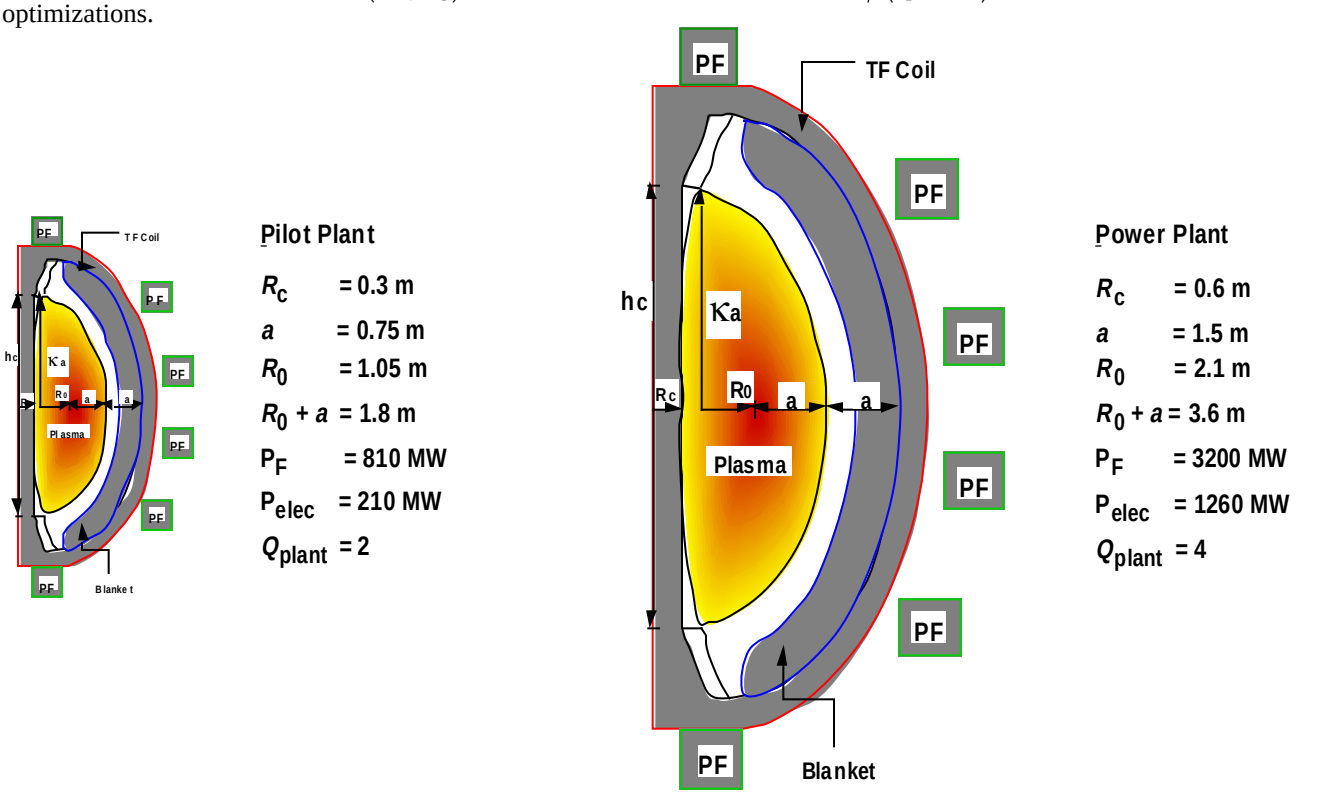

Fig. 1. An ST power plant is about twice the linear dimension of an ST pilot plant. Both cases for A = 1.4, neutron wall load at the blanket 8 MW/m^2, β_T = 62%, β_p = 1.07, f_{bs} = 0.9, κ = 2.5.

$$\beta_T = \frac{0.027\, n_{020}\, T_0}{B_T^2} \quad , \quad \left(T_e = T_i\right) , \tag{3}$$

$$P_F = 1.4\left(\beta_T\, B_T^2\right)^2 V(\mathrm{MW,T,m^3}) \quad . \tag{4}$$

Besides the radius R_c and height h_c of the centerpost, the centerpost current I_c and current density J_c define the problem. λ is the fraction of the centerpost area that is copper. The power P_c is

$$P_c = \frac{\eta_c\, h_c\, I_c}{\lambda\, \pi\, R_c^2} = \frac{\eta_c\, h_c\, J_c^2\, \pi\, R_c^2}{\lambda} \quad . \tag{5}$$

Expressing B_T, V, and $h_c = 2\ a\kappa$ in terms of the basic variables

$$\frac{P_F}{P_c} = \frac{(1.4)(0.2)^4\, \pi^5 \lambda}{\eta_c}\, J_c^2\, \beta_T^2 \times \frac{R_c^4\,(A-1)^2}{A^3}\left(J_c \text{ in MA/m}^2\right) . \tag{6}$$

Since the fusion power rises like β_T^2 it is necessary to construct a relation for the β-limit as a function of aspect ratio. From the definition the quantities involved {using poloidal circumference $c_p = 2\pi a\ [(1 + \kappa^2)/2]^{1/2}$ and $\beta_p \equiv (\mu_0 I_p/c_p)$}, one can obtain

$$\beta_T \beta_p = 25\left(\frac{1+\kappa^2}{2}\right)\left(\frac{\beta_N}{100}\right)^2 \quad . \tag{7}$$

Equation (7) squarely puts one of the major conflicts in present day advanced tokamak design, at any aspect ratio. One wants high β_T for fusion power. One wants high β_p for high bootstrap fraction. But β_T and β_p trade-off against each other, given conventional β-limit scaling $\beta_N = \text{constant}$. The way to increase β_T and β_p *simultaneously* is to increase κ and β_N. We have chosen $\kappa = 2.5$. We have chosen to anticipate a *specific advantage* of low aspect ratio in plasma stability by taking in this paper $\beta_N = 12/A$. Recent full stability analyses (13) for $n = \infty$ ballooning and low-n kinks are supporting this anticipation. In Fig. 2, we show the function $\beta_N = 12/A$ versus A. This function passes through the center of the range of data from DIII–D (14); $\beta_N = 6$, more optimistic than our assumed function, has been achieved transiently and is expected to be stable in steady-state in the operating mode called second stable core VH–mode (SSC-VH) (15) [more recently referred to as negative central shear mode (16)]. Data on beta limits does not exist at low A. But the General Atomics group

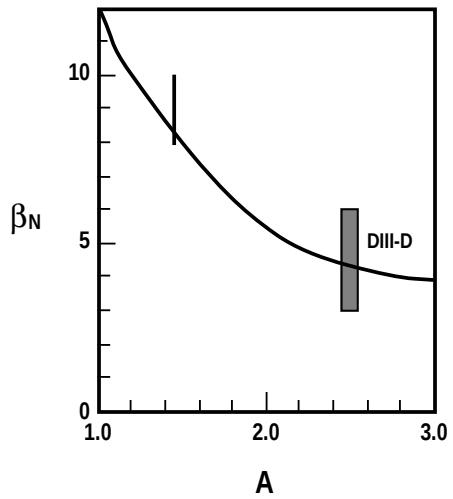

Fig. 2. Assumed relation of $\beta_N = 12/A$. Achieved values in DIII–D experiments are shown at A = 2.5. A range of theoretical calculations from Ref. (13) are shown at A = 1.4.

have obtained equilibria stable to ideal modes at $\beta_N = 8$ to 10 at $A = 1.4$ (13), giving the range shown in the figure. Using β_N = 12/A in Eq. (7) to eliminate β_T in Eq. (6).

$$\frac{P_F}{P_c} = \frac{(1.4)(0.2)^4\, \pi^5 \lambda}{\eta_c}\left(\frac{0.36\left[(1+\kappa^2)/2\right]}{\beta_p}\right)^2 \times J_c^2\, R_c^4\, \frac{(A-1)^2}{A^7} \quad . \tag{8}$$

This last relation, which displays the aspect ratio dependence in the problem explicitly and implies an optimum aspect ratio of 1.4. Taking $A = 1.4$, $\beta_p = 1$, and condensing Eq. (8),

$$\frac{P_F}{P_c} = 1.9\, \lambda\, J_c^2\, R_c^4 \quad . \tag{9}$$

The relation [Eq. (9)] shows a very strong economy of scale in the low aspect ratio approach since $P_F/P_c \propto R_c^4$. Shortfalls in plasma parameters which lower P_F/P_c can easily be made up by making the machine only slightly larger. For example, if we operate at $1/\sqrt{2}$ of the β-limit, then P_F and P_F/P_c are down a factor of two. To recover that factor of two, we only need to make the machine larger by $2^{1/4}$ = 1.19, only a 19% increase in size.

III. CENTERPOST COOLING

Since $P_F/P_c \propto J_c^2$, we need to ask what limits J_c? Centerpost cooling is an obvious candidate but turns out to not be restrictive. The basic reason is that the

centerpost is a short, once-through, water path. Following the development of Montgomery (17), for a water temperature rise of 100°C, a flow velocity of 10 m/s, and $\lambda = 1/2$, we find

$$J_c^2\,(\mathrm{MA/m^2}) = 6.2\times10^4/h_c \quad , \tag{10}$$

Putting this relation for J_c^2 into Eq. (8) we find centerpost gain now is optimized for $A = 1.75$. With $\kappa = 3$ and $A = 1.75$ and $\lambda = 1/2$

$$\frac{P_F}{P_c} = 5560\,R_c^3 \quad . \tag{11}$$

This optimization is to very small machines $(R_c = 0.2\,\mathrm{m})$ with enormous power outputs (11 GW!). Such an optimization is produced from Eq. (10) which will boost the J^2 dependence of P_F/P_c by shrinking h_c and the whole device size. This optimization path leads to high toroidal field (10.5 T) devices because the centerpost cooling limit supports J_c as high as 200 MA/m^2. Such machines are already unrealistically small; the neutron wall loading would be far beyond what blankets could handle. Centerpost cooling is simply not a limitation.

IV. NEUTRON WALL LOADING LIMITS

A neutron wall loading constraint will be the limiting factor in performance. Blanket design studies have already shown 8 MW/m^2 to be at the high end of possibility. We take advantage of the roughly spherical shape of the ST device and assume the neutrons are emitted uniformly onto a sphere of radius $R_0 + 2a$, *i.e.,* the blanket is spaced one minor radius from the edge of the plasma. We compute the actual wall loading for operation at the β-limit.

$$\frac{0.8\,P_F}{A_{wall}} = \frac{(0.8)1.4\,(0.2)^4\pi^6}{4\pi}\left(\frac{0.36\,[(1+\kappa^2)/2]}{\beta_p}\right)^2 \times J_c^4\kappa\,R_c^5\;\frac{(A-1)^3}{A^7\,(A+2)^2} \quad . \tag{12}$$

Equation (12) shows that the family of machines with constant wall loading at some limit is defined by $J_c^4\,R_c^5 = \text{constant}$. With this constraint, the centerpost gain P_F/P_c from Eq. (8) will have the size scaling $R_c^{3/2}$, a much weaker economy of scale than the robust R_c^4 considering only operation at the β-limit with a fixed J_c. We can quickly evaluate a set of machines at the neutron wall loading limit of 8 MW/m^2. Using $\beta_p = 1,\ \kappa = 2.5,\ \lambda = 0.8,\ A = 1.4$ in Eq. (12)

$$J_c^4\,R_c^5 = 1.2\times10^4 \quad . \tag{13}$$

Using this constraint we get a table of devices (Table I). Despite the severity of the wall loading constraint, Table I shows an interesting family of machines, all of small size, but with high gain and fusion power output.

Table I
Devices at an 8 MW/m^2 Neutron Wall Load

R_c (m)	h_c (m)	J_c (MA/m^2)	P_F/P_c	P_c (MW)	P_F (MW)
0.2	3	78	19	49	936
0.3	4.5	60	34	60	2050
0.4	6	33	53	71	3740
0.5	9	25	74	95	7030

In this paper we have treated the plasma elongation κ as a fixed ratio. The "natural" elongation, that elongation which lies at the limit of passive vertical stability afforded by a uniform vertical field (7), rises as A decreases, reaching about 1.9 at A = 1.4 for flat current profiles. Most present tokamaks with elongated cross-sections operate with κ above the passive stability limit, using a nearby conducting structure (the vacuum vessel in the case of DIII–D) to retard vertical drift times to the L/R time of the structure (~1–5 ms in DIII–D) and feedback from the poloidal coils to maintain vertical position stability on longer time scales. The limit to this control approach is reached when the plasma becomes ideal MHD unstable *even in the presence of the conducting structure* (18). Some preliminary calculations indicate that $\kappa = 3$ may be the feedback stability limit at A = 1.4 with peaked current profiles. The maximally stable κ should rise as the current profile is broadened. Hollow current profiles (the negative central shear regime) are required for the high values of β_N we have postulated. From these considerations, our choice $\kappa = 2.5$ is probably a conservative choice of what can be achieved with feedback control.

The ST approach is efficient at shrinking the horizontal dimension of the device, but somewhat at the expense of raising the vertical dimension. We might expect the cost to scale roughly like the volume of the machine, or plasma, and have examined the variation of the plasma volume with κ versus minor radius as we hold constant the centerpost gain P_F/P_C. We find that increasing κ from 2 to 3 is able to effect a factor 2 reduction in plasma and machine volume, providing strong motivation to increase the elongation.

V. INTEGRATED DESIGNS

Since the analysis of the previous section did find an interesting set of machines within the wall loading constraint, we pressed on to construct a complete plant model in a spreadsheet. We document here the relations used in the spreadsheet and display the results as a set of figures later.

A. Approach

The centerpost height is assumed to be $h_c = 2a\kappa$. The current density J_c is assumed and adjusted to give the specified wall loading power. The centerpost is assumed to be 80% copper, λ = 0.8. No correction is made for the temperature dependence of the copper resistivity, $\eta_c = 1.7\times10^{-2}$ $\mu\Omega$m. A water flow velocity V_w = 10 m/s is assumed. The temperature rise is calculated and is never large for the machines shown.

The outer legs of the TF coil are sized to obtain a resistive dissipation equal to a specified fraction $f_R = 0.5$ of the centerpost power. Twelve return legs are taken and the resulting cross-sections are modest (0.2 to 0.6 m on a side). The voltage drop on the return leg is added to the centerpost voltage drop to obtain a total voltage drop on the TF coil, V_{TF}, which ranges from 8 to 7 V for the range of machines to be shown. Since we envision semiconductor power supplies for the TF with an unavoidable internal voltage drop of about 1 V, we take the electrical efficiency of the TF power supply to be 0.9 $\left(1-1\text{V}/V_{TF}\right)$. J_c is adjusted to obtain a specified P_F/A_{wall}. The ratio P_F/P_c is then calculated.

We specify the bootstrap fraction $f_{bs} = 0.9$ and compute $\beta_p = f_{bs}\sqrt{A}$. The β_T is calculated from (7) with β_N = 12/A. Then $I_p/aB_T = 100\,\beta_T/\beta_N$ and $I_p\,(\text{MA}) = aB_T\left(I_p/aB_T\right)$. The safety factor q is always unrestrictive (~6). The product $n_{20}T_{keV}$ is computed from β_T. We assume T_{keV} = 45 keV and calculate the density n_{20}, which ranges from 4 to 2×10^{20} m^{-3}. These densities range from 0.4 to 0.8 times the Greenwald limit $n_{GR} = I_p\,(\text{MA})/\pi a^2$.

We compute the power required to drive the remainder of the current $I_{CD} = I_p(1 - f_{bs})$ following Tonon (19). We compute the volume average density and temperature from the assumed profiles (S_N = 0, S_T = 2]. Then

$$P_{CD} = \frac{\bar{n}\,R_0\,I_{CD}}{\gamma} \quad , \tag{14}$$

where γ is the usual current drive figure of merit for the various current drive schemes (19).

Because these low aspect ratio machines have a low B_T and high n, the rf and NB current drive schemes suffer in efficiency. Hence we looked at helicity injection current drive derived from an electrode as in the HIT experiment (20). Current profiles from HICD tend to be flat so we compute the Ohmic dissipation in the plasma assuming a flat current profile in the presence of a temperature profile given by

$$T_e(r) = T_0\left[1-\left(1-T_b/T_0\right)(r/a)^2\right]^{S_T} \quad , \tag{15}$$

$$P_{OH}\,(\text{MW}) = \frac{0.028\,\pi R_0^2\,I_p^2\ (\text{MA})}{\pi a^2\kappa}\,\frac{1}{T_0^{3/2}}\left(\frac{T_0}{T_b}\right)^2 \quad . \tag{16}$$

We have taken $Z_{eff} = 1$, T_0 = 45 keV, T_b = 200 V. The values P_{HICD} that result range from 30 to 60 MW. The compatibility of HICD with good confinement is an issue.

Because these machines have high power density, they also pose a severe divertor challenge. Taking account of bremsstrahlung and assuming P_{RAD} = 25% of the sum of $P_\alpha + P_{CD}$, we calculate the index of divertor power handling P/R_0 and find values ranging from 100 to 250 MW/m; P/R_0 in ITER is ~40 MW/m. It appears these devices will need to use a radiating mantle to deliver the power to the large area outer wall instead of trying to handle a majority of the power in the small divertor volume.

The viewpoint taken to this point has been to examine operation at the β-limit. Hence we know the stored energy in the plasma. The total heating power $P_\alpha + P_{CD}$ has also been calculated, so we can calculate the energy confinement time required to provide a steady-state at the β-limit. Those confinement times are then compared to the ITER89–P L–mode scaling (21) to define $H = \tau_E/\tau_{89P}$. The absolute energy confinement times are reasonable, ranging from 0.3 to 0.7 s. When these values of τ_E are compared to the ITER L– and H–mode scalings, confusion results. The problem is that these scalings have no basis at $A = 1.4$ and the H–mode scaling predicts a τ_E about half of L–mode at $A = 1.4$, which makes no sense. An H factor of 3.5 in the pilot plant range is required and $H = 2.5$ in the power plant range is required.

We translated the calculated values of heating power, TF coil power, and fusion power into an overall plant electrical efficiency $Q_{\mathrm{PLANT}} \equiv$ gross electrical power output/electrical power to run the plant. The electrical efficiency of the current drive system is taken as $\eta_{\mathrm{CD}} = 0.4$. The electrical efficiency of the TF power system η_{TF} was taken as $0.9\left(1 - 1/V_{\mathrm{TF}}\right)$ as discussed earlier. All other plant systems are assumed to require 7% of the gross electric power generated. So the power recirculating in the plant is

$$P_{\mathrm{RECIRC}} = P_{\mathrm{CD}}/\eta_{\mathrm{CD}} + P_{\mathrm{TF}}/\eta_{\mathrm{TF}} + 0.07\,P_{\mathrm{GROSS,E}} \quad . \tag{17}$$

To compute the gross electric output, a blanket multiplier $M = 1.25$ was taken. It was also assumed that 50% of the power collected as heat $\left(P_{\alpha} + P_{\mathrm{CD,E}} + P_{\mathrm{TF,E}}\right)$ could be taken into the thermal cycle. The efficiency of the thermal cycle was taken as 46%. The gross electric power is

$$P_{\mathrm{GROSS,E}} = \left[M\left(P_{\mathrm{F}} - P_{\alpha}\right) + 0.5\left(P_{\alpha} + P_{\mathrm{CD,E}} + P_{\mathrm{TF,E}}\right)\right]\Big/0.46 \ , \tag{18}$$

$$Q_{\mathrm{PLANT}} = P_{\mathrm{GROSS,E}}/P_{\mathrm{RECIRC}} \quad . \tag{19}$$

The net electric power is $P_{\mathrm{GROSS,E}} - P_{\mathrm{RECIRC}}$.

B. Resulting Machines

The low aspect ratio path does contain a small pilot plant type device and an attractive economy of scale to power plants. All of the designs considered have in common A = 1.4, β_T = 62%, β_p = 1.07, f_{bs} = 0.90, κ = 2.5, neutron power at blanket = 8 MW/m^2.

Figure 3 shows P_F/P_c and Q_{PLANT} versus machine size as gauged by R_c. At the low end, $R_c \sim 0.2$ to 0.3 m, we find devices with $P_F/P_c = 8$ to 14 and $Q_{\mathrm{PLANT}} = 1.3$ to 1.8. Such devices are minimum size and cost pilot plants. At larger $R_c = 0.6$ to 0.7 m, we find a suitable range for a power plant with $P_F/P_c = 40$ to 50 and $Q_{\mathrm{PLANT}} = 3.8$ to 4.4. In Fig. 4, we see the pilot plant makes a fusion power in the range 400 to 800 MW and a net electric power in the range 50 to 200 MW. The power plants make fusion power 3000 to 4000 MW and net electric power in the 1000 to 2000 MW range. These are all small devices. The pilot plant has $R_0 = 0.7$ to 1.0 m and $a = 0.5$ to 0.8 m. The power plants have $R_0 = 2$ to 2.5 m and $a = 1.5$ to 1.8 m.

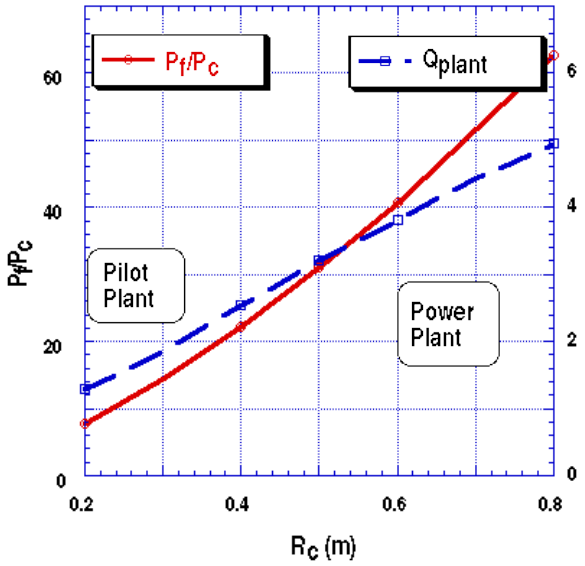

Fig. 3. The ST approach contains a small pilot plant with plant Q = 1–2 and a strong economy of scale to power plants with a plant Q = 4–5.

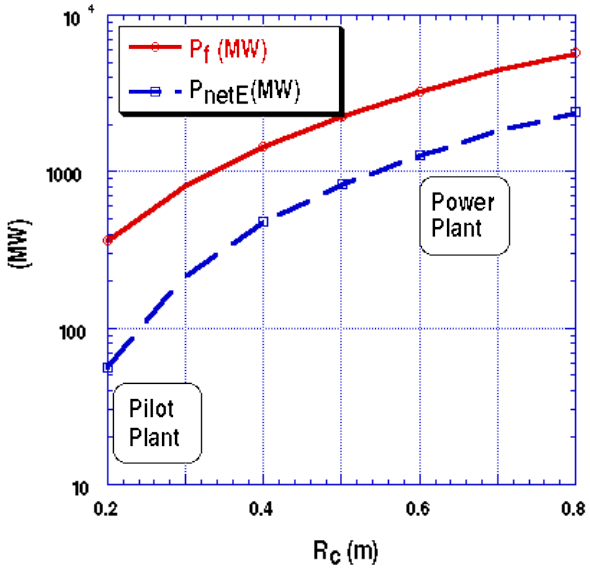

Fig. 4. Pilot plants make 50–250 MW net electric. Power plants make 1000–2000 MW net electric.

The wall loading constraint forces J_c to decrease as R_c increases as shown in Fig. 5. The pilot plants have $J_c = 80$ to 50 MA/m^2 and toroidal fields 2.9 to 2.7 T. The power plants have $B_0 = 2.2$ to 2.1 T and $J_c \sim 20$ MA/m^2, a technically low value that only produces about a 10°C rise in the centerpost cooling water temperature. The centerpost power ranges from 50 MW in the pilot plant to 90 MW in the power plant. The plasma current ranges from 10 to 15 MA in the pilot

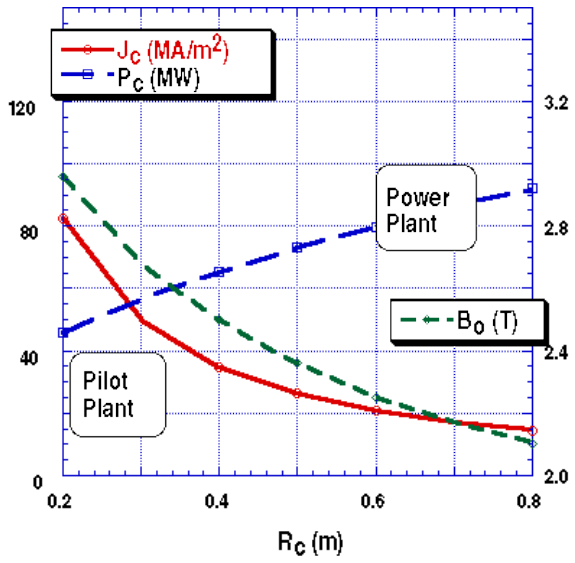

Fig. 5. Allowable neutron wall loading (8 MW/m^2) forces J_C and B_O to decrease with increasing R_C, β_T = 62%, β_p = 1.07, f_{bs} = 0.9.

plant to 25 MA in the power plant. For the overall current drive power, we took the average of the neutral beam and HICD results. The current drive power range is from 40 to 70 MW.

C. Technology Issues

We have calculated the lifetime of the centerpost in the power plant (R_C = 0.6 m case) against the nuclear transmutation induced increase in resistance. We used 2-D distributions of dpa calculated in an R_C = 0.14 m centerpost in a volume neutron source study (22). Fitting those data with a double exponential allowed their use on our larger centerpost. One MW-yr/m^2 produces 10 dpa in the copper surface at the midplane. The change in resistivitry per dpa is 2.8 × 10^{-10} Ω-m/dpa. With an 8 MW/m^2 neutron flux on the centerpost (consistent with 8 MW/m^2 at the outer blanket) we find a 10% increase in one year and, 50% increase in 7 years, and a 100% increase in 22 years. The centerpost changeout time for economic reasons (too high P_C) would be ~7 years.

We also looked at the unusual low voltage, high current semiconductor power supplies needed for the TF coil with a one turn centerpost and 12 return legs. To keep reasonable the transmission line power losses, the power supplies must closely ring the device (4–5 m transmission line lengths) with a floor space requirement of 0.3 m^2/MVA and a 6 m height. The cost for a 12 return leg system for the power plant is about $30–60M and for the power plant is $70–110M.

D. Prospects for Advanced Fuel Burning

The ST approach has a very strong scaling of gain P_F/P_C with machine size (α R_C^4) which quickly leads to absurdly high fusion power output and very high gain in devices of the ITER class burning D-T. The question naturally arises as to whether there is enough excess capacity in the ST at large size to burn advanced fuels like D-He^3 despite their lower reactivity. A D-He^3 system can produce as low as 1% of the neutrons from a D-T system, effectively removing centerpost radiation damage as a design issue. We developed the formula for fusion power from D-He^3 in terms of β.(23) and obtain

$$P_F = 0.0255 \left(\beta_T B_T^2\right)^2 V \text{ (MW, T, m}^3\text{)} \quad . \qquad (20)$$

The D-He^3 fusion power output is 55 times less then the D-T output at the same β_T.

The basic difficulty with realizing an effective D-He^3 system is a surprising one; for systems with high gain, the absolute value of the fusion power produced is too large. To see this, we note from Eq. (7) that since the fusion power from D-He^3 is down by a factor 55 compared to D-T, to get the same gain P_F/P_C we must increase the size of the machine like R_C α $(55)^{1/4}$. Unfortunately from Eq. (4), we find that the fusion power output scales like R_C^7. Hence the ratio of the fusion power in our larger D-He^3 device to the fusion power in our smaller D-T power plant will be

$$\frac{P_{D-He^3}}{P_{D-T}} = \frac{1}{55}\left[(55)^{1/4}\right]^7 = (55)^{3/4} = 20 \quad . \qquad (21)$$

Even though the D-He^3 reactivity is so much lower than D-T, we get 20 times more fusion power out at the same gain P_F/P_C!

This remarkable outcome became quickly apparent from using the modified integrated system design spreadsheet. Of course, to reduce the fusion power, one decreases J_C, but then the gain is also reduced. We have not been able to find a sensible set of parameters for a copper TF coil ST burning D-He^3. One is led to a parameter space with R_C ~ 2.7 m, R_O ~ 9.4 m, a ~ 6.7 m, B_O ~ 2.7 T, and J_C ~ 5.6 MA/m^2. In such systems, the centerpost is absolutely very large and the current density is extremely low. The possibility would seem to exist to easily replace the copper TF coil with a superconducting TF coil and within the space envelope afforded by R_C = 2.7 m easily include a cryostat and neutron shield. This step eliminates the ohmic dissipation in the TF from the power balance and allows a D-He^3 system at a fusion

power output of 11 GW with a plant Q = 4. From this cursory look at burning D-He^3 in an ST device, it would appear there is some possibility in large device sizes if the copper TF coil is replaced with a superconducting TF coil.

VI. SUMMARY DISCUSSION OF KEY ISSUES

We discussed a class of machines with self similar geometry, fixed aspect ratio and elongation, in which case one linear dimension characterizes the device size. We defined the key figure of merit for the ST system as the "centerpost gain," defined as the ratio of fusion power to Ohmic dissipation in the centerpost. Our approach was to examine the ultimate performance of the ST approach by examining operation at the beta limit and the neutron wall loading limit at the blanket. We sought and found systems with that gain P_F/P_C greater than 20 in the belief that a net electric power system could then result. We carried the analysis forward to a full plant calculation [in the manner of Tonon, (19)], and found that we could find power plant systems with overall plant Q in the range 4–5, an effective economic range. We found a very strong size dependence $\left(R_c^4\right)$ of the gain so that any shortfall in fusion power by a factor f or increase in centerpost dissipation by a factor f can be made up by an $f^{1/4}$ increase in the machine size. We found that the cooling of the centerpost imposes no meaningful restriction on the design of ST machines. Apparently the high beta potential of the ST is so great that the physics of this device will not determine its size. Instead, the limit to neutron flux into the fusion blankets was found to limit the size of the device. An aggressive assumption of 8 MW/m^2 at the blanket then leads to the small pilot plant and power plant possibilities that we have found. We have chosen an elongation of 2.5 in our design cases. This elongation probably lies above the limit of passive vertical stability but below the limit of vertical stability using feedback. An increase of elongation from 2 to 3 can effect a factor of two reduction in the plasma (and so probably) the machine volume.

We demanded a 90% bootstrap fraction, according to the simple estimate $f_{bs} = \sqrt{\varepsilon}\,\beta_p$. This simple estimate is optimistic; calculatons in Ref. (13) suggest a coefficient of ~0.75 should be used, but the theory for bootstrap current at low A is evolving. We calculated the current drive power requirements for the various standard schemes to drive the remaining 10% of the current. We also evaluated helicity injection current drive, which is essentially edge current drive at the edge temperature.

Although more detailed system calculations should be done in the areas outlined above and for other aspects of the problem, the physics advances over today's database that are called for to make the ST path attractive involve a much greater reach than the level of inaccuracy in our approach to this assessment. We briefly summarize the needed physics progress elements along the ST path.

1. High $\beta_N \sim 10$ at $A = 1.4$ and $\beta_T > 50\%$. The relation $\beta_N(A)$ must be determined first theoretically and then experimentally with the specific numerical goals above as targets.

2. High Elongation. The upper limits to $\kappa(A)$ must be established for both passive and feedback stabilized operation.

3. Confinement Database. Projections of present scalings to the low A regime are not useful.

4. Non-Inductive Startup. In order to build thermonuclear ST devices without an OH coil, an experimental demonstration of the non-inductive startup of a ~1 MA ST is needed.

5. Bootstrap Fraction and Alignment. Because the ST is inherently a high plasma current device, high bootstrap fraction is necessary.

6. Divertor Operation. The adequacy of divertor configurations that are achievable without a divertor coil and/or an inner leg must be explored.

7. Non-Inductive Current Drive. The low A regime without generally low B_T and high n_e poses specific challenges to find applicable current sustainment techniques.

8. Plasma Current Limitations. The lower bound on $q(A)$ needs to be established experimentally.

VII. CONCLUSIONS

In this paper, we find that within this ST concept, it appears (see Fig. 1) possible to design a pilot plant that would only be the size of the present DIII–D tokamak and yet still produce some net electric power. At double the size of the pilot plant we find full 1–2 GW net electric power plants with acceptable economics. The ST approach thus has the two key features of an executable commercialization strategy: a low cost pilot plant that can attract commercial cost sharing at an affordable level and with minimal financial risk, and a strong economy of scale leading to power plants that are still small on an absolute scale.

The pilot plant is the key to this strategy. With its small size, it offers a possibility to make net electric

power for a total project cost under $1B. Commercial parties might be able to participate in such a project on a cost sharing basis with the government share still dominant . To justify any commercial participation, the device must be accepted by the commercial parties as a pilot plant. The most elementary definition of a pilot plant seems to be a device that makes electricity but does not necessarily sell any of it. The power output is low, 50–200 MW net electric, rather than trying to initiate a new technology at the multi-gigawatt level. The plant Q, defined as the ratio of gross electric power to internal recirculating power is only 1–2. The low plant Q will be acceptable in a pilot plant if the concept has a strong economy of scale. The ST size scaling is very strong; the ratio of fusion power to the Ohmic dissipation in the copper TF coil magnet scales as the fourth power of the linear dimension. Consequently, we easily find small power plants with economically acceptable recirculating power (plant Q ~ 4–6, net electric power 1–2 GW). The ST approach can progress from the pilot plant to the power plant just by doubling the linear dimensions of the device with no changes in technology. The ST is a simplified tokamak with no hard to service inboard blankets, shields, PF or OH coils. Indeed, because the TF coil is copper, it can be jointed and so afford easy complete dissassembly of the machine for service. The ST concept offers high elongation and a natural divertor without a divertor coil. Finally, because that ST pilot plant is a full net electric and tritium producer, it will provide a full exercise of the siting and licensing process, but again at a low cost, low financial risk scale. The fact that a viable concept for a pilot plant exists is the principal attraction of the ST approach to government to commercial transition.

VIII REFERENCES

1. Y-K. M. Peng and D. J. Strickler, "Features of Spherical Torus Plasmas," Nucl. Fusion **26**, 769, (1986).

2. Y-K. M. Peng and J. B. Hicks, "Engineering Feasibility of Tight Aspect Ratio Tokamak (Spherical Torus) Reactors," *Proc. of the 16th Symposium on Fusion Technology*, London, September 3–7, 1990.

3. Y-K. M. Peng, et. al., "Summary of Workshop on Establishing the Physics Basis Needed to Access the Potential of Compact Toroidal Reactors," *Fusion Technol.* **29**, (1995) 210.

4. A. C. Darke, et. al., "The Mega Amp Spherical Tokamak," *Proc. of the 16th Symposium on Fusion Energy*, Champaign-Urbana, Illinois, 1995.

5. J. H. Chrzanowski, H. M. Fan, P. J. Heitzenroeder, M. Ono, J. Robinson, "Engineering Overview of the National Spherical Tokamak Experiment," *ibid*.

6. FRC Staff, "USTX — The University Spherical Tokamak Experiment," DOE/ER/542-41-159 (1996).

7. A. Sykes, "Progress on Spherical Tokamaks," *Plasma Phys. and Contr. Fusion* **36**, B93 (1994).

8. Y-K. M. Peng, et. al., "Physics Progress Towards Compact Tokamak Reactors with Normal Conducting Toroidal Field Coils," *Proc. of the 15th International Confercence on Plasma Physics and Controlled Nuclear Fusion Research*, Seville, Spain, 1994 (International Atomic Energy Agency, Vienna, 1995) Vol. 2, p. 643.

9. T.C. Hender, et. al., "Tight Aspect Ratio Tokamak Reactors," *ibid*.

10. R.D. Stambaugh, et al., "The Spherical Tokamak Path to Fusion Power," General Atomics Report GA-A22226 (1996) submitted to *Fusion Technology*.

11. *NRL Plasma Formulary* NRL/PU/6790-94-265, J. D. Huba, editor (1994).

12. J. D. Callen, B. A. Carreras, R. D. Stambaugh, "Stability and Transport Procession Tokamak Plasmas," *Phys. Today* **45**, 34 (1992).

13. R. L. Miller, Y. R. Lin-Liu, A. D. Turnbull, V. S. Chan, and L. D. Pearlstein, "Stability for Bootstrap-Current Driven Low Aspect Ratio Tokamaks," General Atomics Report GA-A22321, to be submitted to *Phys. of Plasmas*.

14. J. R. Ferron, L. L. Lao, T. S. Taylor, Y. B. Kim, E. J. Strait, D. Wróblewski, "Improved Confinement and Stability in the DIII–D Tokamak Obtained Through Modification of the Current Profile," *Phys. Fluids B* **5**, 2532 (1993).

15. R. D. Stambaugh, et al., "DIII–D Program Overview," *Plasma Phys. and Contr. Nucl. Fusion Research* **1**, 83 (1994).

16. E. A. Lazarus, et al., "Higher Fusion Power Gain With Pressure Profile Control in Strongly-Shaped DIII–D Tokamak Plasmas," General Atomics Report GA–A22292 (1996) submitted to *Phys. Rev. Lett*.

17. D. B. Montgomery, *Solenoid Magnet Design*, (Wiley-Interscience, New York, 1972).

18. R. D. Stambaugh, L. L. Lao, E. A. Lazarus, "Relation of Vertical Stability and Aspect Ratio in Tokamaks," *Nucl. Fusion* **32**, 1642 (1992).

19. G. Tonon, "Current Drive Efficiency Requirements for an Attractive Steady-State Reactor," *Proc. of the Workshop on Tokamak Concept Improvement*, Varenna, Italy, August 1994, p. 233.

20. P. N. Yushmanov, et al., "Scalings for Tokamak Energy Confinement," *Nucl. Fusion* **30**, 1999 (1990).

21. F. Ryter, et al., "Expression for the Thermal H–Mode Energy Confinement Time Under ELM-Free Conditions in Deuterium," *Nucl. Fusion* **33**, 979 (1993).

23. G. H. Miley, H. Towner, N. Ivich, "Fusion Cross Sections and Reactivities," University of Illinois Report COO-2218-17, June 1994.